

Darcy and post-Darcy flows within different sands

Écoulements darciens et post-darciens dans différents sables

IMAM WAHYUDI, *Assistant Professor, Civil Engineering Faculty of Unissula Semarang, Jl. Kaligawe KM-04, Semarang, Indonesia*

AGNÈS MONTILLET, *Assistant Professor, Chemical Engineering Laboratory, Nantes University, IUT, BP420, 44606 Saint-Nazaire cedex, France*

ABDERAHMANE O.A. KHALIFA, *Assistant Professor, Civil Engineering Laboratory, Nantes University, IUT, BP420, 44606 Saint-Nazaire cedex, France*

ABSTRACT

The present paper reports a study conducted to examine several sands with a large spread of particle size in order to validate the modelling of both Darcy's and Forchheimer's law parameters, which could be applied to any kind of sand. An experimental set-up has been specially conceived to generate hydraulic gradients within fine sands higher than 600. We also present an attempt at using a capillary-type flow model to determine structural parameters of sand and predict pressure gradients. The specific surface areas calculated appear to be consistent with surface areas estimated from screening experiments. Similarly, tortuosity values calculated from pressure drop experiments stand within the range of values found in the literature, measured using an alternative method, the conductometric method.

Using one dimensionless equation of the capillary-type flow model, a single value of the pore Reynolds number makes it possible to determine, whatever the porous medium, the limits of Darcy's flow regime. This Reynolds number value is 4.3.

RÉSUMÉ

Dans ce travail, nous proposons l'étude expérimentale de plusieurs sables présentant une importante étendue granulométrique dans le but de valider une modélisation des paramètres des lois de Darcy et de Forchheimer, généralisables à tous les types de sables. Un dispositif expérimental est spécialement développé pour générer des gradients hydrauliques dans les sables fins, supérieurs à 600. Ce travail présente une première tentative d'utilisation d'un modèle d'écoulement capillaire pour déterminer les paramètres de structure de sables et de prédire les gradients de pressions dans ces sables. On montre que les surfaces spécifiques calculées à partir du modèle sont proches de celles issues de la distribution granulométrique. Dans le même ordre d'idées, les valeurs de la tortuosité calculées par le modèle sont proches de celles issues de la littérature, déduites d'une méthode alternative: la conductimétrie.

Ce même modèle d'écoulement de type capillaire, basé sur une écriture adimensionnelle, permet de déterminer la limite de validité de la loi de Darcy, à partir d'une valeur unique du nombre de Reynolds, quel que soit le sable. Cette valeur du nombre de Reynolds est de 4.3.

Introduction

Modelling of flows within porous media has been the subject of many studies conducted over the past few decades. Modelling of flows within sand can be applied to various domains such as civil engineering, hydrogeology and oil engineering. In oil exploitation, sands are natural water or hydrocarbon reservoirs, the recovery of which requires a good knowledge of the behaviour of fluid within the granular medium according to the flow velocity. In civil engineering, these researches are applied to the study of internal flows within earth and rock structures (McCorquodale et al., 1985; Martin, 1990; Shih, 1991; Hansen 1992) and to the problems of similarities of flow parameters in centrifuged geotechnical small-scale models, within which very large hydraulic gradients are often found (Babendreier, 1991; Poux, 1997; Khalifa et al., 2000).

The most relevant progresses have been made with Darcy's (1856) and Forchheimer's (1901) studies on flow phenomena within sands, the laws of whom are still references today. Many studies have been conducted on these natural materials since. Most, however, have been restricted to the study of Darcy's laminar and linear domain. Recently, modelling progresses of flows within unconsolidated, granular media rely mostly on experimental works using homogeneous, spherical, artificial media (Ergun,

1952; Comiti and Renaud, 1989). The extrapolation of these models to wide particle-size distributed natural media requires, therefore, specific studies. Some researches have been carried out on coarse, natural materials such as gravel and rock (McCorquodale et al., 1985; Martin, 1990; Shih, 1991; Hansen, 1992; Burchart et al., 1991; Bingjun et al., 1998). Few, on the other hand, have been conducted to examine post-Darcy's flows within sands (Babendrier, 1991; Menand, 1995) while most are restricted to macroscopic characteristics (permeability) and can be applied, consequently, only to the sands studied by the authors.

The present paper describes the experimental study of different types of sand with a large particle-size distribution in order to validate a model, which could be applied to any kind of sand. The experimental set-up is particularly suitable for the study of these materials since, besides the classical Darcy's domain, it can be used to examine the post-Darcy's domain thanks to the hydraulic gradients generated, which may exceed 600 for fine sands. The modelling approach presented here is centred on the characterisation of macroscopic parameters (pore diameter, tortuosity and porosity of the medium, etc.), on the one hand, and on the determination of the range of validity of Darcy's linear law based on a unique criterion common to all sands, on the other hand. The capillary model applied here has been developed by Comiti and

Revision received September 20, 2000. Open for discussion till December 31, 2002.

Renaud (1989) and was first used for artificial, porous media (packing of spheres and plates).

We begin the present paper with the introduction of the capillary model used, followed by the description of the experimental set-up and finally with the presentation of the experimental results.

Piezometric pressure drop modelling

The attempts to model piezometric pressure drops measured when studying flows within sands, sandstones and shaly sands are numerous. Because of its numerous applications, the Darcy's flow domain is more often investigated, most of the research works focusing on the prediction of the permeability coefficient (Revil and Cathles, 1999; Hamilton, 1997). Nevertheless, some authors have extended their experimental works to the study of non linear, laminar flow regimes (Fancher and Lewis, 1933; Ahmed and Sunada, 1969), and made some attempts to lay down the principle of pressure drop modelling.

Ahmed and Sunada (1969), in particular, propose an interpretation of the Navier-Stokes equation, applied to the case of flow through pores, in order to obtain a dimensionless general equation:

$$H = \frac{1}{R} + 1 \quad (1)$$

With H, a friction factor, defined as: $H = g \frac{k}{d} \frac{i}{v_o^2}$

And R, a Reynolds number, defined as: $R = \frac{\rho v_o d}{\mu}$

The permeability, k, and the characteristic length of flow, d, are both estimated from the hydraulics measurements. They are constant for a given porous medium. The authors consider these parameters to represent the physical properties of the pore structure. The importance of this work lies in its capacity to represent experimental data obtained with different sands with a single equation, Equation (1), whatever the sand. The classical dimensionless representations, also based on two parameters, found until then in the literature (Beavers and Sparrow, 1969, for instance), could gather the experimental data in the Darcy flow regime only.

Comiti and Renaud (1989) propose a capillary-type modelling of the piezometric pressure drop through unconsolidated porous media consisting of anisotropic particles. This model is primarily developed to estimate the proportion of overlapping surface areas in packed beds of flat plates. It was successfully tested with uniform spheres and, then, also applied to highly porous, reticulated media (Montillet 1995). This model is based on the representation of the porous medium by a set of identical cylindrical tortuous pores with a diameter of pore, d_{pore} :

$$d_{pore} = \frac{4n}{(1-n)Avd} \quad (2)$$

where n is the porosity and Avd is the dynamic specific surface

area defined as the ratio of the total pore surface area, exposed to fluid flow, to the volume of solid.

The mean velocity in pores is: $v_{pore} = \frac{v_o \tau}{n}$ (3)

where τ is the tortuosity defined as the ratio of the mean length of the flow path to the crossed thickness of the porous medium.

In Comiti and Renaud (1989), a complete equation of the model, expressed as a Forchheimer's law, is given, which takes into account a correction for the wall effects. The correction is based on two points : a different value of the friction factor must be considered at the wall and the calculation of the specific surface area must be corrected for the surface area of the wall. In the current study, wall effects can undoubtedly be ignored because of the high value of the ratio of the cell diameter to the particle diameter (approximately 100).

After that, the Forchheimer-type equation of the model becomes:

$$i = a v_o^2 + b v_o \quad (4)$$

with

$$a = 0.0968 \tau^3 Avd \frac{(1-n)}{g n^3} \quad (5)$$

and

$$b = 2 \mu \tau^2 Avd^2 \frac{(1-n)^2}{\rho g n^3} \quad (6)$$

A dimensionless equation of this model is then (Comiti et al. 2000) :

$$f_{pore} = \frac{16}{Re_{pore}} + 0.194 \quad (7)$$

with

$$f_{pore} = \frac{\Delta P}{h} \frac{2 n^3}{\tau^3 \rho Avd (1-n) v_o^2} \quad (8)$$

and

$$Re_{pore} = \frac{4 \rho \tau v_o}{\mu (1-n) Avd} \quad (9)$$

In the same way as the development of Ahmed and Sunada (1969), this model also includes two parameters and can represent experimental data obtained with different media with a single equation. However, the physical meaning of the presently calculated parameters, Avd and τ , has been previously demonstrated to be more effective. As mentioned above, the model of Comiti and Renaud (1989) has been successfully tested with uniform spheres and reticulated media: the dynamic specific surface area and the tortuosity calculated with the model from hydraulic measurements have been compared with the calculated static specific surface area of the spheres, to the static specific surface area of reticulated media determined with image analysis and to the tortuosity values determined with the electrical method. Both calculated parameters were in close agreements with those determined independently.

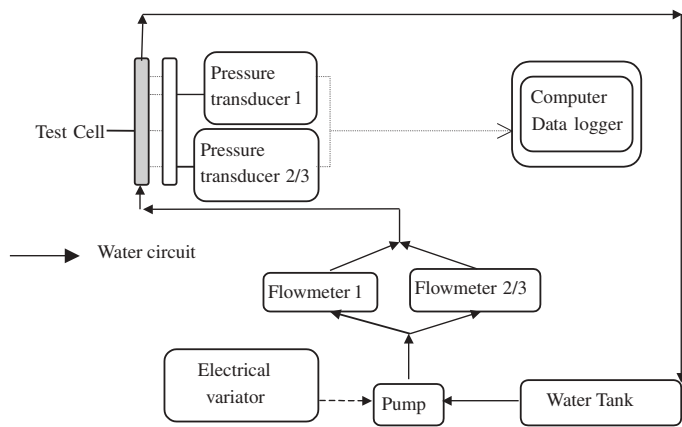


Fig. 1 Schematic diagram of the set-up

The objective of this research is to use the model of Comiti and Renaud (1989) to calculate A_{vd} and, then, compare it with the static specific surface area obtained from sand screening analysis.

Experimental results and analysis

Experimental set-up and method

The experimental set-up, the schematic diagram and the photograph of which are presented in Figure 1 and 2, respectively, consists of both a hydraulic device and a measurement device (Wahyudi, 1998).

The hydraulic device consists of a pump inverting the flow of water from a 200-liter tank through the material placed in the test-

ing cell. When flowing out of the cell, water is forced back into the tank. The temperature is monitored at a quasi-constant value: 20.0 ± 0.5 °C. Temperature sensors are placed in the tank, at the entrance and at the exit of the test cell. Then the values of the water density, ρ , and of the water viscosity, μ , are quasi constant during the tests ($\rho = 998.23$ kg m⁻³ and $\mu = 1.008$ Pa s).

An electronic variator is used to control the speed of rotation of the pump and indirectly, the flowrate desired. Thanks to the variator the pump works optimally and reduces potential losses of energy, which might raise the level of the temperature of the water and of the noise in the laboratory. During the test, the valves are wholly open to avoid vibrations and keep the flowrate steady. The testing cell is equipped with five pressure tappings (Figure 3):

- a bottom pressure tapping,
- 3 pressure tappings located 2.5 cm above the bottom pressure tapping with a 120-angle spacing to control the horizontal homogeneity of the bed,
- an upper pressure tapping located 5 cm above the bottom tapping.

Some valves are used to select the pressure tappings and the differential pressure gauge suiting the best measurement range.

The measurement bench consists of three electromagnetic flowmeters and four differential pressure gauges regulated by a valve set. The different measurement ranges of these devices are complementary and can be used to cover all the measurements accurately. The design features of the equipment are presented in Table 1.

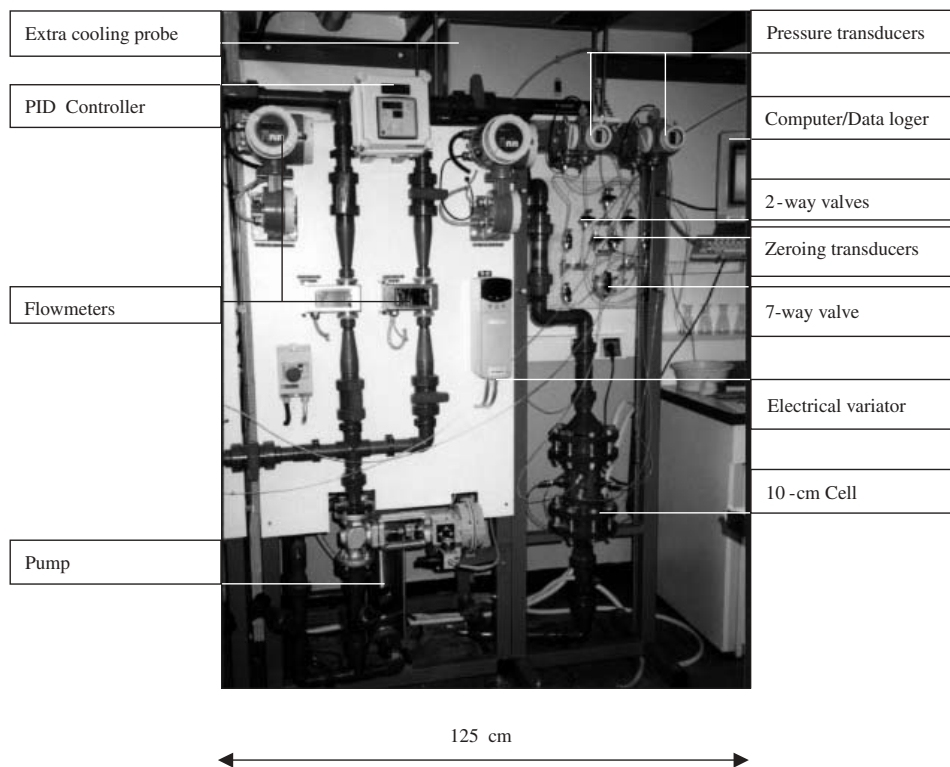


Fig. 2 Photograph of the experimental set-up

Table 1. Design features of the equipment

DESIGNATION	DESCRIPTION	CHARACTERISTICS
Electromagnetic Flowmeter 1	Endress+Hauser Promag 33	$Q_{max} = 0.452 \text{ m}^3/\text{h}$ $\pm 0.5\%$ of the full range
Electromagnetic Flowmeter 2	Endress+Hauser Promag 33	$Q_{max} = 6.360 \text{ m}^3/\text{h}$ $\pm 0.5\%$ of the full range
Electromagnetic Flowmeter 3	Endress+Hauser Promag 33	$Q_{max} = 0.113 \text{ m}^3/\text{h}$ $\pm 0.5\%$ of the full range
Differential pressure gauge 1	Silicon membrane Deltabar S PMD 230	$\Delta P_{max} = 0.25 \cdot 10^5 \text{ Pa}$ $\pm 0.1\%$ of the full range
Differential pressure gauge 2	Silicon membrane Deltabar S PMD 230	$\Delta P_{max} = 1.60 \cdot 10^5 \text{ Pa}$ $\pm 0.1\%$ of the full range
Differential pressure gauge 3	Silicon membrane Deltabar S PMD 235	$\Delta P_{max} = 1 \cdot 10^5 \text{ Pa}$ $\pm 0.1\%$ of the full range
Differential pressure gauge 4	Silicon membrane Deltabar S PMD 235	$\Delta P_{max} = 6 \cdot 10^5 \text{ Pa}$ $\pm 0.1\%$ of the full range
Cell	Cylindrical, transparent p.v.c.	diameter: 10 cm length: 10 cm
Pump	Centrifugal pump	Flowrate: $8 \text{ m}^3/\text{h}$ pressure: 16 bars

The sand was packed as homogeneously as possible using the pluviation method with a constant 1.2 m height of fall. Satisfactory repeatability of the bulk densities was achieved throughout the experiments. The bed porosity is calculated knowing the cell volume and the mass of sand (the sand density is measured with a pycnometer). The material flooding is implemented according

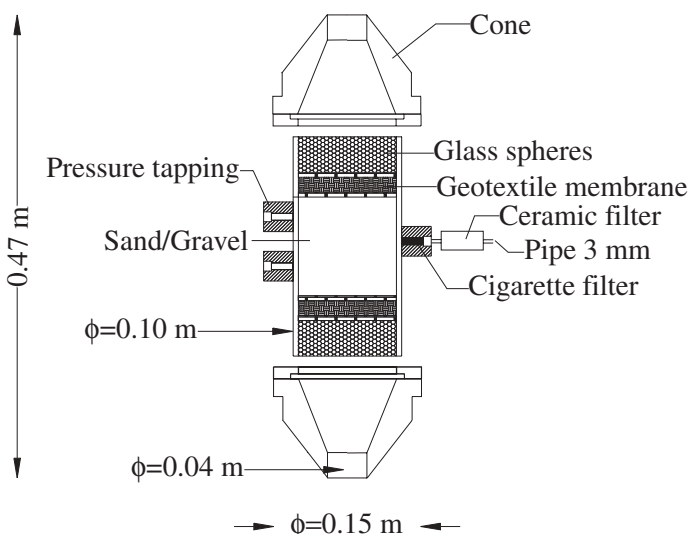


Fig. 3 Cross section of the cell

to an experimental protocol to eliminate air bubbles inside the set-up:

- the material is saturated with water by increasing progressively the water level in the cell with a very low flowrate,
- water is, then, circulated at its maximum flowrate during several hours to flush potential air bubbles from the system,
- pressure gauges are flushed and balanced,
- the experiments are then conducted only if the pressure homogeneity in the bed is verified (horizontally and vertically).
- repeated measurements with both low and high rates of flow are carried out. When, at a given flowrate, measurements proved to be constant, the system is considered as correctly deaired and the actual test can begin.
- Measurements are first carried out at increasing flow rates followed by decreasing rates to prevent superimposition or detect possible hysteresis.

Experimental results

Sand screening characterisation

Sand screening characterisation is carried out on samples of five different French sands of various geological and geographical origins (Fontainebleau, Hostun, Labenne, Rheu and Loire sands). The results of the sand screening test are shown in the form of cumulative weight percent v.s. mesh size (Figure 4). In Figure 5, the surface area frequency of the sand fraction retained in each sieve is presented as a function of the sieve opening. The surface area frequency is calculated considering that the sand particles are spherical. Both figures give a clear idea of the wide particle-size distribution, and of the main features of these distributions. Some of the sands tested have relatively narrow particle-size distributions (Fontainebleau and Labenne sands) whereas the others are characterised by wider particle-size distributions.

Pressure drop results

The experimental data, presented in Figure 6, are expressed as the hydraulic gradient versus the superficial velocity. The experimental coefficients of Equation (4), a and b, are obtained by optimising the mean relative error, ERM, between the experimental and the calculated values. The values of a and b are

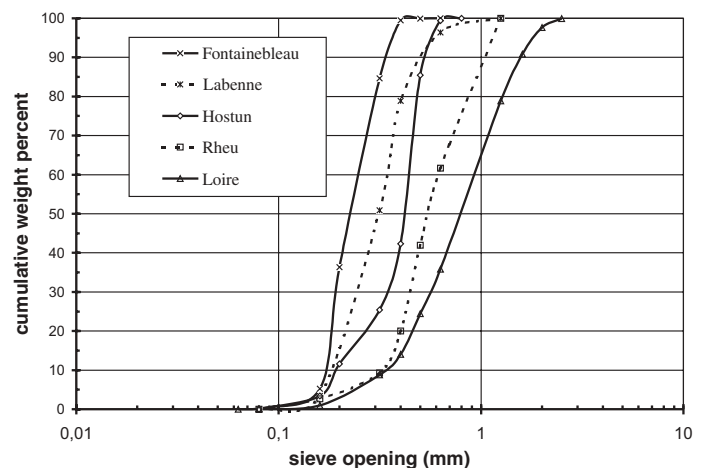


Fig. 4 Sand screening curves

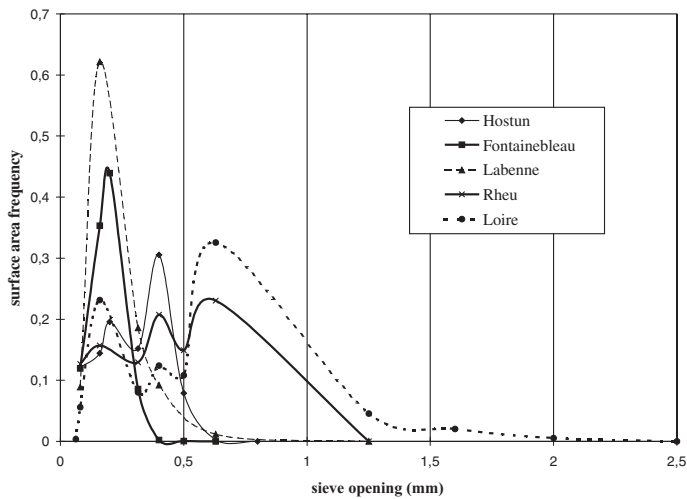


Fig. 5 Surface area frequency of sands

given in Table 2, as well as the number of data and the mean relative error:

$$ERM = \frac{1}{p} \sum_{j=1}^p \frac{|i_{exp}(j) - i_{cal}(j)|}{i_{exp}(j)} \quad (10)$$

We have minimised the absolute error as it immediately gives an order of magnitude of the mean scatter between experimental and calculated data. The experimental values are perfectly aligned when they are plotted as $i/v_0=f(v_0)$, then using rms error or absolute error criteria gives very closed a and b values.

Table 2 Values of the experimental coefficients of the Forchheimer's law.

Sand:	b (s m ⁻¹)	a (s ² m ⁻²)	p, number of data	ERM (%)
Fontainebleau	53 10 ²	19.4 10 ²	57	1.1
Labenne	24.9 10 ²	10.6 10 ²	52	2.0
Hostun	23.9 10 ²	16.1 10 ²	107	1.8
Rheu	15.9 10 ²	18.7 10 ²	38	1.5
Loire	5.94 10 ²	7.96 10 ²	76	1.3

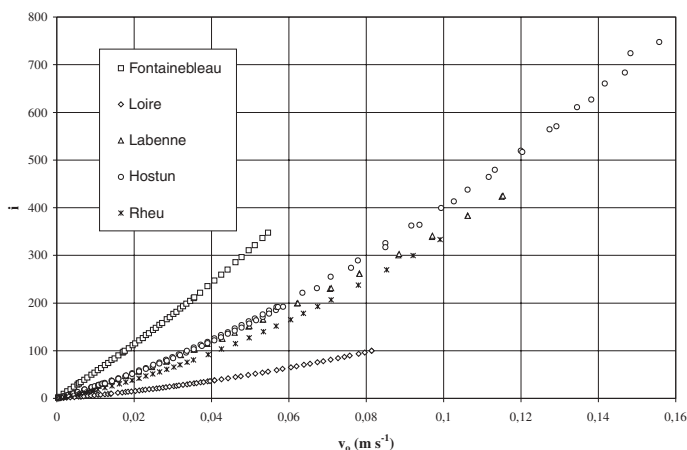


Fig. 6 Hydraulic gradient (i) versus superficial velocity (v₀) for sands

The two structural parameters of the model, A_{vd} and τ , are then calculated from the respective expressions of a and b given by Comiti and Renaud's model (Equations 5 and 6). The values of sand bed porosity, the values of τ and A_{vd} and the estimated values of the static specific surface area of the sands, A_{vs} , as well as the scatter between A_{vd} and A_{vs} , are plotted in Table 3. A_{vs} is estimated assuming that the sand particles are spherical, and using the mean surface area diameter of particles obtained from the screening tests:

$$A_{vs} = \frac{6}{d_m} \quad (11)$$

with

$$d_m = \frac{\sum_{j=1}^p m_j}{\sum_{j=1}^p \frac{m_j}{d_j}} \quad (12)$$

The estimated values of A_{vs} and the calculated values of A_{vd} are in close agreement. The scatter is lower than 10%, except for the sand from the Loire river. In view of the rough estimation of A_{vs} , which is probably affected by a larger uncertainty than A_{vd} from an experimental point of view, the scatter between the two parameters can be considered as small. Moreover, apart from the Loire sand, the values of A_{vd} and A_{vs} are so close that it may indicate that surface areas do not overlap.

The larger difference between A_{vd} and A_{vs} in the case of the Loire sand can be attributed to its wider particle size distribution and its greater variability with respect to chemical composition and shape of the particles. In particular, this sand contains a non negligible amount of flat plate-shaped broken shells. The presence of such particles is, on the one hand, increasing the uncertainty on the determination of A_{vs} , and, because of the possible overlapping of particles in the bed, accounts for the physical difference between the static and the dynamic specific surface areas. The reliability of the tortuosity cannot be determined as easily since literature data on the subject are scarce. Moreover, this parameter can be characterised by multiple definitions and determined by different experimental means. In our opinion, the tortuosity factor can be, here, compared with the electrical determinations of the tortuosity as reported by Carman (1961). In Carman (1961), some tortuosity values achieved with conductometric measurements conducted in sands and in mixtures of glass particles by different authors are reported. Considering the porosity range of our sand beds, the reported tortuosities are within the range 1.51-1.71, for fairly narrow particle size distributions. For a wider particle-size distribution and lower porosity (n is about 0.25), a tortuosity value of 2.0 has been measured. These results indicate that our values are contained within a reasonable range.

Table 3 Structural parameters of the sand beds.

Sand:	N	Avs (m ⁻¹)	Avd (m ⁻¹)	Scatter (%)	τ
Fontainebleau	0.384	33 000	36 200	9.6	1.71
Labenne	0.376	28 700	27 000	6.0	1.50
Hostun	0.392	21 200	22 400	5.7	1.93
Rheu	0.377	15 800	14 500	8.3	2.24
Loire	0.318	12 600	8 500	32	1.65

Dimensionless representation of data – Proposal of a critical Reynolds number defining the scope Darcy’s regime limits

According to the dimensionless equation of the model presented above, Equation (7), the data are plotted in Figure 7 as f_{pore} versus Re_{pore} . As mentioned before, the relevance of this kind of representation is to gather experimental data with a single equation whatever the porous medium. Therefore, a single value of the pore Reynolds number can determine the limits of Darcy’s regime, considering a chosen error. For instance, if a tolerance of 5% for the deviation of Darcy’s law is accepted, then the corresponding critical pore Reynolds number is: $Re_{pore}^{critic} = 4.3$

For selected tolerances of 1% and 10%, the critical pore Reynolds number values are respectively 0.83 and 9.2.

It is not easy to compare these results with the literature, since many definitions of the Reynolds number can be found in the literature. For example, the particle Reynolds number and the interstitial Reynolds number are currently used to characterise the flow in porous media. On the other hand, and as previously mentioned in Comiti and al. (2000), Dybbs and Edwards (1984) suggested experimental critical interstitial Reynolds number ranged between 1 and 10. Comiti et al (2000) are giving the interstitial Reynolds number range corresponding to $Re_{pore} = 4.3$ and calculated for different particle shapes : it is comprised between 1 and 8.

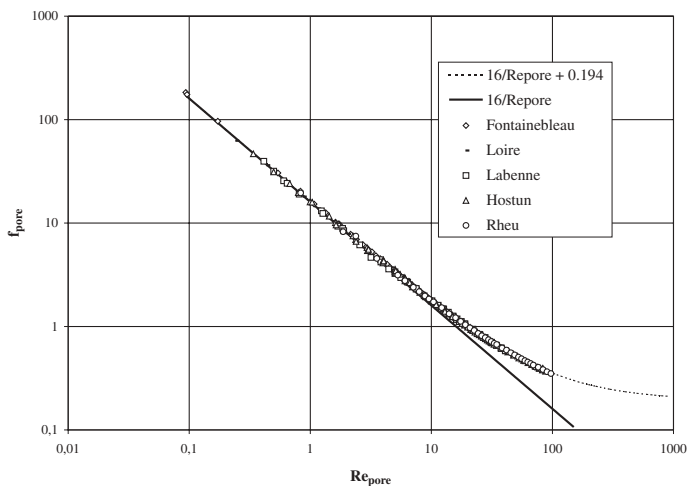


Fig. 7 Friction factor (F_p) versus Reynolds pore number (Re_{pore})

Conclusion

The objective of this research was to examine the use of a capillary-type flow model to determine structural parameters of sand and critical Reynolds number corresponding to the limit of validity of Darcy’s law. The specific surface areas calculated are consistent with surface areas estimated from screening experiments. Similarly, tortuosity values calculated from pressure drop experiments are within the range of values found in the literature and measured using an alternative method, the conductometric method.

Using one dimensionless equation of the capillary-type flow model, a single value of the pore Reynolds number makes it possible to determine, whatever the porous medium, the limit of Darcy’s flow regime. The Reynolds number value is 4.3 for five sands geographically different.

In a next step, our research work will focus on the study of the potential of the tortuosity and permeability predictions from particle size distribution and shape characteristics of sand.

Acknowledgements

This present research work is backed by the French Department of Research and Technology and is conducted in collaboration with the Laboratoire de Génie des Procédés (LGP) and the Laboratoire Central des Ponts et Chaussées (LCPC). The assistance and cooperation of Dr Garnier (LCPC) and Pr. Comiti (LGP) are sincerely appreciated. Special thanks to Mr. Coué for his involvement in the perfecting of the experimental set-up.

Nomenclature

- a coefficient of Equation 4, s² m⁻²
- Avd dynamic specific surface area, m⁻¹
- Avs static specific surface area, m⁻¹
- b coefficient of Equation 4, s m⁻¹
- d characteristic dimension, m
- d_j opening dimension of the j sieve, m
- d_m mean surface area diameter of particles (Equation 12), m
- d_{pore} diameter of pores (Equation 2), m
- ERM mean relative error, dimensionless
- f_{pore} pore friction factor, dimensionless
- g gravity acceleration, m s⁻²
- h height of bed, at which the pressure drop is measured, m
- H friction factor as defined by Ahmed and Sunada (1969), dimensionless
- i hydraulic gradient, dimensionless
- i_{cal} calculated hydraulic gradient (Equation 4), dimensionless
- i_{exp} measured hydraulic gradient, dimensionless
- k permeability (Equation 1), m²
- m_j mass of particles retained in the j sieve, kg
- n porosity, dimensionless
- ΔP pressure drop, Pa
- R Reynolds number as defined by Ahmed and Sunada (1969), dimensionless
- Re_{pore} pore Reynolds number, dimensionless

v_o	superficial velocity, $m\ s^{-1}$
v_{pore}	mean velocity in pores, $m\ s^{-1}$

Greek letters

μ	fluid dynamic viscosity, Pa s
ρ	fluid density, $kg\ m^{-3}$
τ	tortuosity, dimensionless

References

- AHMED, N., and SUNADA, D.K., (1969). Non linear Flow in porous media. *J. of the HYDRAULICS DIVISION – Proceedings of the American Society Engineers*, HY6, 1847-1857.
- BABENDREIER, C.A., (1991). Grain size effect on scales in centrifuge modelling of saturated steady state seepage in particulate media. *Master of Science Thesis, University of Maryland, USA*, 63p.
- BEAVERS, G.S., and SPARROW, E.H., (1969). Non-Darcy flow through fibrous porous media. *J. of Applied Mechanics*, n°12, 711-714.
- BINGJUN LI, GARGA V.K., DAVIES M.H., (1998). Relations for non-Darcy flow in rockfill. *Journal of Hydraulic Engineering*, ISSN 0733-9429, Vol. 124, n° 2, 206-212.
- BURCHART, H.F., and CHRISTENSEN, C., (1991). On stationary and non-stationary porous flow in coarse granular materials. *MAST G6-S Project 1, Wave action on and in coastal structures*, Aalborg university, Denmark, 1991, 67p.
- CARMAN, P.C., (1961). L'écoulement des gaz à travers les milieux poreux. *Bibliothèque des Sciences et des Techniques nucléaires*, P.U.F., 52.
- COMITI, J., and RENAUD, M., (1989). A new model for determining mean structure parameters of fixed beds from pressure drops measurements: application to beds packed with parallelepipedal particles. *Chem. Eng. Sci.*, 44, 1539-1545.
- COMITI, J., SABIRI N.E., and MONTILLET, A., (2000). Experimental characterization of flow regimes in various porous media – III: limit of Darcy's or creeping flow regime for Newtonian and purely viscous non-Newtonian fluids. *Chem. Eng. Sci.*, 55, 3057-3061.
- DARCY, H., (1856). Les fontaines publiques de la ville de Dijon, Ed. Victor Dalmont, Paris, France.
- ERGUN, S., (1952). Fluid flow through packed columns. *Chemical Engineering Progress*, Vol. 48., n° 2, 89-94.
- FANCHER, G.H., and LEWIS, J.A., (1933). Flow of simple fluids through porous materials. *Industrial and Engineering Chemistry*, 25(10), 1139-1147.
- HAMILTON, R.T. (1997). Darcy constant for multisized spheres with no arbitrary constant. *AIChE Journal*, 43(3), 835-836.
- HANSEN, D., (1992). The behaviour of flow through rockfill dams. *The degree PhD*, University of Ottawa, Canada, 355 p.
- KHALIFA, A., GARNIER, J., THOMAS, P. and RAULT, G. (2000). Scaling laws of water flow in centrifuge models. *International Symposium on Physical Modelling and Testing in Environmental Geotechnics*, La Baule, France, May
- MARTIN, R. (1990). Turbulent seepage flow through rock-fill structures. *Int. Water Power and Dam Construction*, 03, 41-45.
- MCCORQUODALE, J.A., HANNOURA, A.A., (1985). Rubblemounds: numerical modelling of wave motion. *ASCE Journal of the Waterway, Port, Coastal and Ocean Division*, Vol. 111, n° 5, 800-816.
- MENAND, S., (1995). Etude expérimentale des limites de validité de la loi de Darcy sous forts gradients dans les sables fins. *Master of Science Thesis*, LCPC-Université de Nantes, France, 61 p.
- MONTILLET, A., (1995). Fiabilité de la détermination de paramètres structuraux de mousses synthétiques à partir de mesures de chutes de pression. *Récents Progrès en Génie des Procédés*, 9, 125-130.
- POUX, A., (1997). Etude des écoulements dans les sols granulaires centrifugés, *Master of Science Thesis*, University of Nantes, France, 116p.
- REUIL A., CATHLES L.M., (1999). Permeability of shaly sands. *Water Resources Research*, 35(3), 651-662.
- FORCHHEIMER, P., (1901). Wasserbewegung durch Boden. *Z. Ver. Deutsch. Ing.*, Vol. 45, 1782-1788.
- SHIH, R.W.K., (1991). Permeability characteristics of rubble materials, New formulae. *Proc. ICCE Delft*, 2: 1499-1512.
- WAHYUDI, I. (1998). Steady and unsteady flow through saturated granular soils. *Ph. D. Thesis*, University of Nantes, France, 193 p.